CHAPTER 2

Materials and Methods

2.1. Introduction

This chapter involves in depth about the materials and experimental methods use for the synthesis of fluorescent carbon quantum dots (CQDs). Addition to this, the present chapter also conferred the general idea about the various characterization techniques like Transmission Electron Microscopy (TEM), Selected Area Electron Diffraction pattern (SAED), Fourier Transform-Infrared (FT-IR) Spectroscopy, X-Ray Diffraction (XRD), X-Ray Photoelectron Spectroscopy (XPS), UV-visible Spectroscopy, Fluorescence Spectrophotometer and Zeta potential. (Malvern Zetasizer). The experimental procedures used for the preparation of CQDs have also been discussed in this chapter. Further, the optimization and applications of CQDs as peroxidase-mimetic enzyme activity and as a sensor for the sensing of Ascorbic acid, Hydrogen peroxide, Fe (III), Tyrosine (Tyr) are also enclosed in this chapter. Addition to this, Current chapter also deals with the cell viability test on different cell line and applied as a cell imaging agent. The details about the determination of fluorescence QY have also been covered in this chapter. The preparations of stock solutions of different analytes for their applications have been explained broadly in this chapter.

2.2. Materials

The organic solvent and chemicals required for the synthesis and applications of CQDs were AR grade and utilized as received with no further purifications. These are point out in Table 2.1. In addition, throughout the experiment, distilled water was used.

Table2.1. List of chemicals

S. No.	Name	Chemical formula	Physical state	Manufacturer
1	3,3′,5,5′Tetramethylbenzidine(TMB)	$[\text{-}C_6H_2(CH_3)_2\text{-}4\text{-}NH_2]_2$	solid	Sigma Aldrich
2	Hydrogen peroxide	H_2O_2	liquid	SD Fine-Chem Ltd.
3	Potassium bromide	KBr	Solid	Avra Chemicals, India
4	Potassium iodide	KI	solid	Avra Chemicals, India
5	Glucose	$C_6H_{12}O_6$	solid	Avra Chemicals, India
6	Ascorbic acid	$C_6H_8O_6$	solid	Avra Chemicals, India
7	Cinnamic acid	$C_9H_8O_2$	solid	Avra Chemicals, India
8	Benzoic acid	$C_7H_6O_2$	solid	Avra Chemicals, India
9	Oxallic acid	$C_2H_2O_4$	solid	Avra Chemicals, India
10	Adipic acid	$C_6H_{10}O_4$	solid	Avra Chemicals, India
11	Tartaric acid	$C_4H_6O_6$	solid	Avra Chemicals, India
12	Citric acid	$HOC(COOH)(CH_2COOH)_2$	solid	Avra Chemicals, India
13	Uric acid	$C5H4N_4O3$	solid	Avra Chemicals, India
14	Methanol	CH_3OH	liquid	SD Fine-Chem Ltd.
15	Ethanol	C_2H_5OH	liquid	SD Fine-Chem Ltd.
16	Isopropyl alcohol	$(CH_3)_2CHOH$	liquid	SD Fine-Chem Ltd.
17	Benzoquinone	$C_6H_4O_2$	liquid	SD Fine-Chem Ltd.
18	Acetone	$(CH_3)_2CO$	liquid	SD Fine-Chem Ltd.
19	Dimethyl sulphoxide	$(CH_3)_2SO$	liquid	SD Fine-Chem Ltd.
20	Trichloromethane	$CHCl_3$	liquid	SD Fine-Chem Ltd.
21	Dimethyl sulphoxide-d6	$(CD_3)_2SO$	liquid	Merk
22	Deuterium oxide	D_2O	liquid	Merk
23	Hydrochloric acid	HCl	liquid	SD Fine-Chem Ltd.
24	Sulphuric acid	H_2SO_4	liquid	SD Fine-Chem Ltd.
25	Nitric acid	HNO_3	liquid	SD Fine-Chem Ltd.
26	Sodium acetate	CH_3COONa	solid	SD Fine-Chem Ltd.
27	Sodium hydroxide	NaOH	solid	SD Fine-Chem Ltd.
28	Sodium Chloride	NaCl	solid	Alfa Aesar
29	Potassium Chloride	KCl	solid	Alfa Aesar
30	Sodium Nitrate	$NaNO_3$	solid	SD Fine-Chem Ltd.
31	Potassium Nitrate	KNO_3	solid	SD Fine-Chem Ltd.
32	Aluminium Nitrate	$Al(NO_3)_3.9H_2O$	solid	SD Fine-Chem Ltd.
33	Ferric Nitrate	$Fe(NO_3)_3 \cdot 9H_2O$	solid	Sigma Aldrich
34	Ferric Chloride	$FeCl_3$	solid	Sigma Aldrich
35	Ferrous Chloride	$FeCl_2$	solid	Sigma Aldrich
36	Aluminium Chloride	$Al\ (NO_3)_3$	solid	Sigma Aldrich
37	Lead nitrate	$Pb(NO_3)_2$	solid	SD Fine-Chem Ltd.
38	Manganese nitrate	$Mn(NO_3)_2.6H2O$	solid	Sigma Aldrich
39	Chromium nitrate	$Cr(NO_3)_3.9H2O$	solid	Sigma Aldrich
40	Potassium dichromate	$K_2Cr_2O_7$	solid	Sigma Aldrich
41	Nickel nitrate	$Ni(NO_3)_2 \cdot 6H_2O$	solid	Sigma Aldrich

42	Cobalt nitrate	$Co(NO_3)_2 \cdot 6H_2O$	solid	Sigma Aldrich
43	Copper nitrate	$Cu(NO_3)_2 \cdot 2.5H_2O$	solid	Sigma Aldrich
44	Zinc nitrate	$Zn(NO_3)_2 \cdot 6H_2O$	solid	Sigma Aldrich
45	Cadmium nitrate	$Cd(NO_3)_2 \cdot 4H_2O$	solid	Sigma Aldrich
46	Mercuric nitrate	$Hg(NO_3)_2.H_2O$	solid	Sigma Aldrich
47	Magnesium chloride	$MgCl_2$	solid	Alfa Aesar
48	Arsenic trioxide	As_2O_3	solid	Merk
49	Arsenic pentaoxide	$As_2O_5 \cdot xH_2O$	solid	Merk
50	Silver Nitrate	$AgNO_3$	Solid	Merck
51	Antimony oxide	Sb_2O_3	solid	Alfa Aesar
52	Tyrosine (Tyr)	$C_9H_{11}NO_3$	solid	Avra Chemicals, India
53	Glycine (Gly)	$C_2H_5NO_2$	Solid	Avra Chemicals, India
54	Alanine (Ala)	$C_3H_7NO_2$	Solid	Avra Chemicals, India
55	Valine (Val)	$C_5H_{11}NO_2$	Solid	Avra Chemicals, India
56	Isoleucine (Ile)	$C_6H_{13}NO_2$	solid	Avra Chemicals, India
57	Leucine (Leu)	$C_6H_{13}NO_2$	solid	Avra Chemicals, India
58	Methionine (Met)	$C_5H_{11}NO_2S$	solid	Avra Chemicals, India
59	Phenylalanine (Phe)	$C_9H_{11}NO_2$	solid	Avra Chemicals, India
60	Tyrosin (Tyr)	$C_9H_{11}NO_3$	solid	Avra Chemicals, India
61	Trptophan (Trp)	$C_{11}H_{12}N_2O_2$	solid	Avra Chemicals, India
62	Serine (Ser)	$C_3H_7NO_3$	solid	Avra Chemicals, India
63	Threonine (Thr)	$C_4H_9NO_3$	solid	Avra Chemicals, India
64	Asparagine (asn)	$C_4H_8N_2O_3$	solid	Avra Chemicals, India
65	Glutamine (Gln)	$C_5H_{10}N_2O_3$	solid	Avra Chemicals, India
66	Cysteine (Cys)	$C_3H_7NO_2S$	solid	Avra Chemicals, India
67	Proline (Pro)	$C_5H_9NO_2$	Solid	Avra Chemicals, India
68	Glutamic acid (Glu)	$C_5H_9NO_4$	Solid	Avra Chemicals, India
69	Lysin (Lys)	$C_6H_{14}N_2O_2$	Solid	Avra Chemicals, India
70	Arginine (arg)	$C_6H_{14}N_4O_2$	Solid	Avra Chemicals, India
71	Glutathione (GSH)	$C_{10}H_{17}N_3O_6S$	Solid	Avra Chemicals, India
72	Polyethylene-imine	$(C_2H_5N)_n$	liquid	Sigma Aldrich
73	Quinine sulphate	$C_{40}H_{50}N_4O_8S$	solid	Merk
74	Dulbecco's Modified Eagle's medium	*******	liquid	CELLclone, Genetix Biotech, Asia Pvt. Ltd.
74	Fetal bovine serum	*******	liquid	Gibco (Fetal Bovine Serum, E.U. Approved (SouthAmerican Origin) by life technologies
75	SH-SY5Y neuroblastoma cell line	*******	liquid	National Centre for Cell Science (NCCS), Pune, India

2.3. Method

2.3.1. Synthesis of CQDs

The CQDs were synthesized by bottom up approach through hydrothermal method. First of all, precursor molecules were appropriately dissolved in distilled water and then poured the suspension into Teflon-lined stainless steel autoclave chamber and kept in hydrothermal oven for 2-5 hours at high temperature. After completion of the reaction, the vessel was cooled naturally at room temperature and the obtained brown color solution was filtered. After then, to remove large and agglomerate particle, the filtrate was centrifuge at 10 to 20,000 rpm for 10 to 15 minutes. Finally, the pure CQDs were obtained by filtering the supernatant solution through the dialysis membrane and syringe filter. The detail synthesis procedures of CQDs are stated in chapter3, 4 and 5 under experimental section.

2.4. Preparation of standard solution

2.4.1. Preparation of standard solution of 3,3′,5,5′-Tetramethylbenzidine (TMB)

First of all, we have prepared the stock solution of TMB with 1x 10^{-2} M concentration via dissolving 24.0 mg of TMB in 10 mL of ethanol in a volumetric flask. After then, by using serial dilution of stock solution, we obtained the desired concentration of TMB in ethanol.

2.4.2. Preparation of standard solution of Ascorbic acid (AA)

By dissolving 1.76 mg of AA in 10 mL of distilled water, the stock solutions of AA with the concentration of (1x 10-2 M) were prepared. Further, by using serial dilution method, the lower concentrations of AA were obtained.

2.4.3. Preparation of standard solution of other reducing agents

The stock solutions of other reducing agent like various amino acids were prepared by dissolving appropriate quantity of each amino acid in distilled water in similar manner. The stock solution of Tyr (concentration 1x 10^{-2} M) was prepared by dissolving 0.90 mg tyrosine in 10 mL distilled water.

2.4.4. Preparation of standard solution of Fe^{3+}

The stock solution of Fe^{3+} with concentration of 1x 10^{-2} M were prepared by dissolving 16 mg of $FeCl_3$ was dissolved in 10 mL of ultrapure water in volumetric flask. The desired concentrations of Fe^{3+} solution were obtained from the stock solution by serial dilution method.

2.5. *In vitro* cell imaging study

2.5.1. Cell line

The cell imaging application of CQDs were carried out on SH-SY5Y neuroblastoma cells.

2.5.2. Cytotoxicity assay

To determine the cytotoxicity of as-synthesized GB-CDs, 3-(4,5-dimethylthiazol-2-yl)-2,5- diphenyltetrazolium bromide (MTT) assay was performed on SH-SY5Y neuroblastoma cells. SH-SY5Y neuroblastoma cells were incubated in Dulbecco Modified Eagles Medium (DMEM) and seeded into 96-well cell culture plates. The details are given in chapter 4.

2.6. Calculations

2.6.1. Determination of quantum yield (QY)

The QY of fluorescent CQDs was determined with respect to a standard solution of quinine sulphate (QY = 54% at 340 or 360 nm excitation). The absorbance (below 0.1) and the

integrated intensity of the quinine sulfate solution in 0.1 M H_2SO_4 were also measured. For fluorescent CQDs, the equivalent measurements were performed with similar parameters and QYs were determined using **equation 2.1.**

$$QY = QY_{Ref} \cdot \frac{I}{A} \cdot \frac{A_{Ref}}{I_{Ref}} \cdot \frac{\eta^2}{\eta^2_{Ref}} \qquad \textbf{2.1}$$

Where QY and QY_{ref} are quantum yield of GB-CDs and reference respectively, I is the integrated intensity, A is the absorbance and η is the refractive index (η^2/η^2_{ref} =1) of the solvent.

The details about the intensity and absorbance of quinine sulfate and fluorescent CQDs are given in table 3.1, 4.1 and 5.1of chapter 3, 4 and 5 respectively.

2.6.2. Determination of limit of detection (LOD)

The minimum concentration of an analyte in a sample that can be consistently detected is called limit of detection (LOD). It is determined by using the following **equation 2.2.**

$$LOD = 3\sigma/s \qquad \textbf{2.2}$$

Where "s" denotes the slope of the linear curve and σ represents the standard deviation.

2.6.3. Determination of Stern-Volmer constant

The Stern-Volmer quenching constant was determined by using **equation 2.3.**

$$F_0 / F = 1 + k_{sv}.[Q] \qquad \textbf{2.3}$$

Where F_0 represents the FL intensity of fluorescent CQDs, F is the FL intensity of CQDs in the presence of quencher (Tyr), Q is the concentration of quencher, and k_{sv} symbolize quenching constant.

2.7. Characterization Technique

The as synthesized fluorescent CQDs were characterized through various instrumental techniques which are discussed below.

2.7.1. Transmission Electron Microscopy (TEM)

To analyze in detail about morphology, particle size and crystallographic structure of the specimen, transmission electron microscopy (TEM) is utilized. In TEM technique, high energy electrons beams (up to 300 kV) interact with the ultrathin spacemen. Because of this interaction of the electrons transmitted throughout the specimen an image is formed. An imaging device, like a fluorescent screen, is used to magnify the image or a sensor like charge coupled device (CCD) is used to detect the image. The basic principle of TEM is similar to light microscope but in TEM electron is used instead of light. Since the electrons exhibited dual characteristics i.e. behaves as particle as well as wave nature and the de Broglie wavelength of electrons are considerably smaller than that of light and thus have superior resolution capacity. These allow the instrument's operator to observe fine element which is tens of thousands time smaller than the smallest resolvable particles in a light microscope. TEM is used in physical, chemical and biological sciences as a major analysis method. Because of absorption of electrons as well as thickness and composition of the materials, TEM image is contrast at smaller magnifications. The intensity of the image is modulated by complex wave interactions at higher magnifications

and requiring expert analysis of observed images. Therefore, to observe modulations in crystal orientation, chemical identity, electronic structure and regular absorption based imaging, alternate modes of use permit for the TEM.

Thermionic (tungsten filament or lanthanum hexaboride) or field emission (tungsten filament) electron gun is use to emits the electrons in a typical operational TEM. The area of the illuminated samples and the illumination aperture is control by a set of condenser lenses. The major purpose of the objective lens is the formation of image or diffraction pattern **(Fig. 2.1).** There are two mode of specimen observation in the working principle of TEM, first one is image mode and another one is diffraction mode (Fig. 2.1). The image mode includes bright field imaging and dark field imaging. When the image of a thin sample is produced via the electrons without diffraction, then this is called bright field imaging and when a diffracted beam is used for imaging, called dark field imaging.

In this research work, the TEM analyses of CQDs were carried out on TECNAI 20 G2-Electron Microscope operate at accelerating voltage 200 kV (Fig. 2.2). The samples for TEM analysis were ready by mount the dilute solution of the samples on carbon coated TEM grid and dried underneath table lamp for 5 h after that vacuum dried overnight.

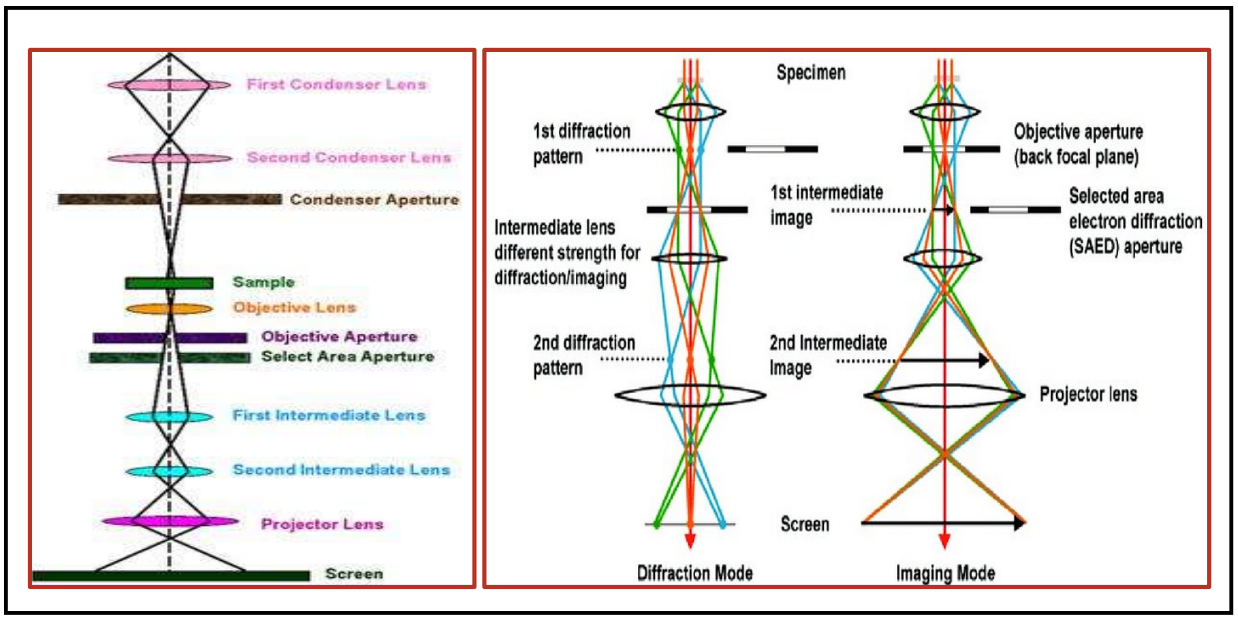

Figure 2.1 Schematic diagrams with working principle of TEM and two different operation mode of TEM.

.

Figure 2.2 Typical image of Transmission Electron Microscope (TEM).

2.7.2. Fourier Transform Infrared (FT-IR) Spectroscopy

FT-IR spectroscopy is utilized for quantitative and qualitative analysis of organic compounds including molecular structure, molecular environment, and chemical bonding. Presence of different functional groups in molecules or compounds is also identifying by FT-IR spectroscopy. Michelson interferometer is used for the working principle of FT-IR which includes beam splitter, a fixed mirror and a movable mirror that translate back and forth specifically. The beam splitter is strike by radiation of source and separate into two beams. First beam goes to the static mirror after transmitted through the beam splitter while second beam reflected the beam splitter to the moving mirror. The radiation is reflected back to the beam splitter by the fixed and moving mirrors. Further, some radiation is transmitted and some is reflected at the beam splitter, because of this one beam passed through the sample , detected by the detector and on computer, spectra are display and the second beam reverse to the source (Fig. 2.3).

In our research work, the FT-IR spectra were carried out on the instrument "Perkin Elmer Spectrum 100" which was equipped with mid-infrared (M-IR) source of radiation. KBr window is used to pass the radiation sources and LiTaO3 detector collects the transmitted data and spectrum was demonstrated in transmitted mode. For the preparation of pellets of the sample, mixed the sample with KBr in 1:100 ratios and scanned the sample pellets in the range of 400-4000 cm^{-1} with the scan speed 0.2 cm/second and spectral resolution of 4.0cm^{-1}.

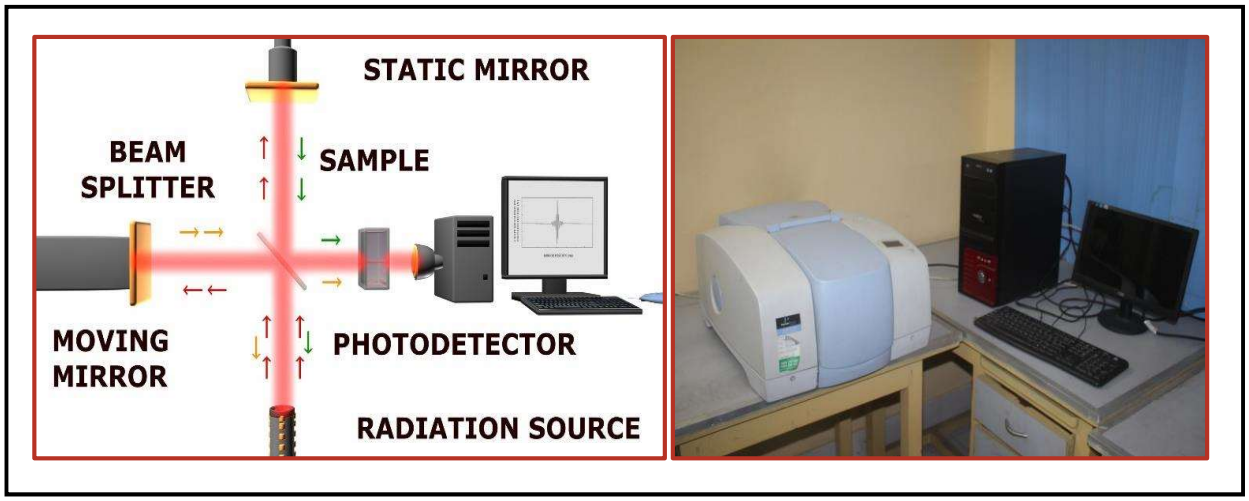

Figure 2.3 Demonstration of working principle of FT-IR and its Photograph.

2.7.3. Ultraviolet-visible (UV-vis) Spectroscopy

The UV–vis spectroscopy is an absorption spectroscopy or reflectance spectroscopy which work in the region of ultra-violet (200-400 nm) and visible (400 - 765 nm). When a beam of light is passed through a sample then it may be absorbs, transmits or reflects over a particular range of wavelength. Usually on sample, light of certain wavelength is illuminated, that absorbs a definite amount of incident light energy and transmits the rest of energy which is identify by photo detector, that registers the absorbance of the sample. To show the relationship between incident light (I_o) and transmitted light (I_t) following (Equation 2.4 and 2.5) are used.

Transmittance (T) = I_t/I_{ob} (2.4)

Transmittance rate (T%) = It/Io * 100 (2.5)

The negative logarithm of the transmittance is the absorbance (A)

Absorbance (A) = - log T = log (1/T) = log (I_o/I_t) = -kcl (2.6)

Where I_t is intensity of transmitted radiation, I_o is the intensity of incident radiation, k is the proportionality constant and l is the path length of the cuvette in cm. From equation 2.5, it can be seen that absorbance is directly proportional to the concentration of sample (Beer's Law) and optical path length (Lambert Law). So, the basic principles of UV-vis absorption spectroscopy are based on Lambert−Beer law. If the optical path length of cuvette is 1 cm and sample concentration is 1 mol/L, then the proportionality constant is called the molar absorption coefficient and denoted by the symbol ε. Beer-Lambert's Law is stated by following formula:

$$\log_{10}\left(\frac{I0}{It}\right) = \varepsilon cl \qquad \textbf{(2.6)}$$

The unit of molar absorption coefficient ε is mol^{-1} dm^3 cm^{-1}.

To quantitatively determine various analyte like conjugated organic compound, transition metal ions, and biological macromolecules, UV-vis spectroscopy is utilized. When UV-vis radiation is absorbed , then excitation of the π electron and nonbonding electron occurs which goes to higher antibonding orbital and following four possible type of electronic transition results as σ–σ* > n–σ* > π–π* > n–π*. Though, most of the transitions involves only π→π*, n→σ* and n→π* transitions.

The UV-vis spectrophotometer includes various apparatus like Light Sources (UV and VIS), sample holder, monochromator (wavelength selector), a detector; signal processor and readout. Generally, deuterium arc lamp is used as the light source for UV-region and tungsten lamp for visible region.

In our research work, UV-vis absorption spectra was aquired on "EVOLUTION 201 Thermo scintific" using 1 cm path length quartz cuvettes in 200–700 nm wavelength range. The graphic diagram and UV- vis spectrophotometer photograph are illustrated in (Fig. 2.4).

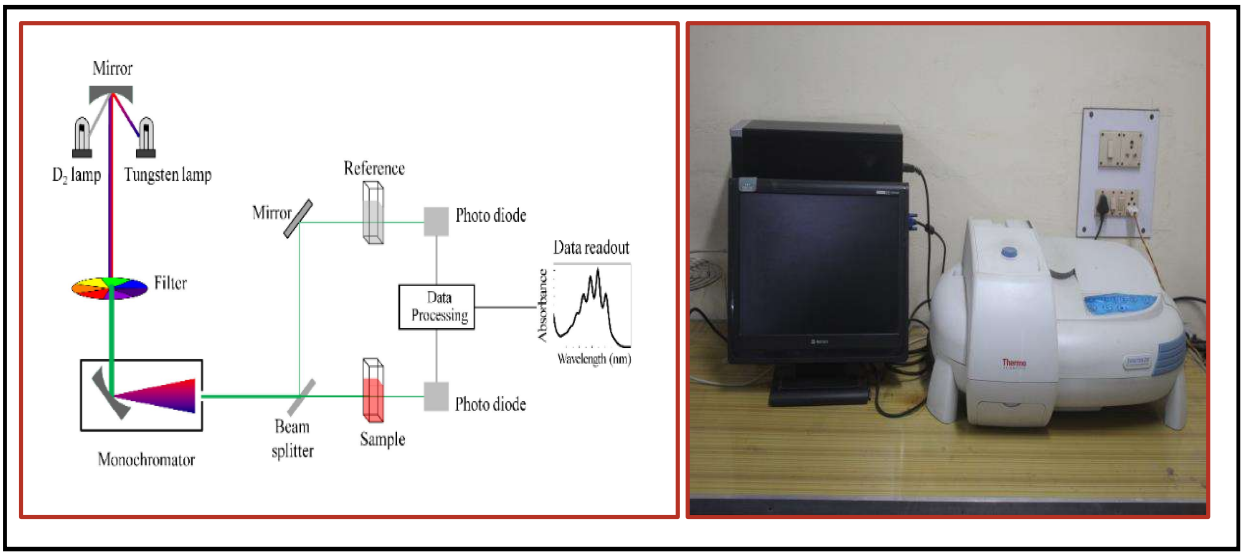

Figure 2.4 Illustration of working principle of UV-visible spectroscopy and their photograph.

2.7.4. Fluorescence Spectroscopy

For inquiring the electronic structure of materials, fluorescence spectroscopy is one of the most adaptable, nondestructive, highly sensitive spectroscopy techniques. To measure the fluorescence or emission intensity, fluorescence spectrophotometer is used. The spectral content of the sample permit to determine their concentrations. Furthermore, when record the

fluorescence, the excitation, emission or both wavelengths might be scanned and monitored the alteration of signal with time, temperature, polarization and concentration. Fluorescence spectroscopy is rather different from absorption spectroscopy since in absorption spectroscopy, there is transition from ground state to excited state, whereas in fluorescence spectroscopy there is transition from excited state to the ground state. Fluorescence spectra is a graph of intensity of emission against some given excitation wavelength. The excitation wavelength is the wavelength at which molecule exhibited maximum absorbance that provides a more intense emission at a longer wavelength. The key components of fluorescence spectrometer include wavelength selectors, light source, sample illumination, detector and data readout. In fluorescence spectrometer, the radiation source used is Xenon arc lamp Figure 2.5.

In our research work, we have used Varian Cary Eclipse fluorescence spectrophotometer for the fluorescence spectrum of CQDs (Fig. 2.5).

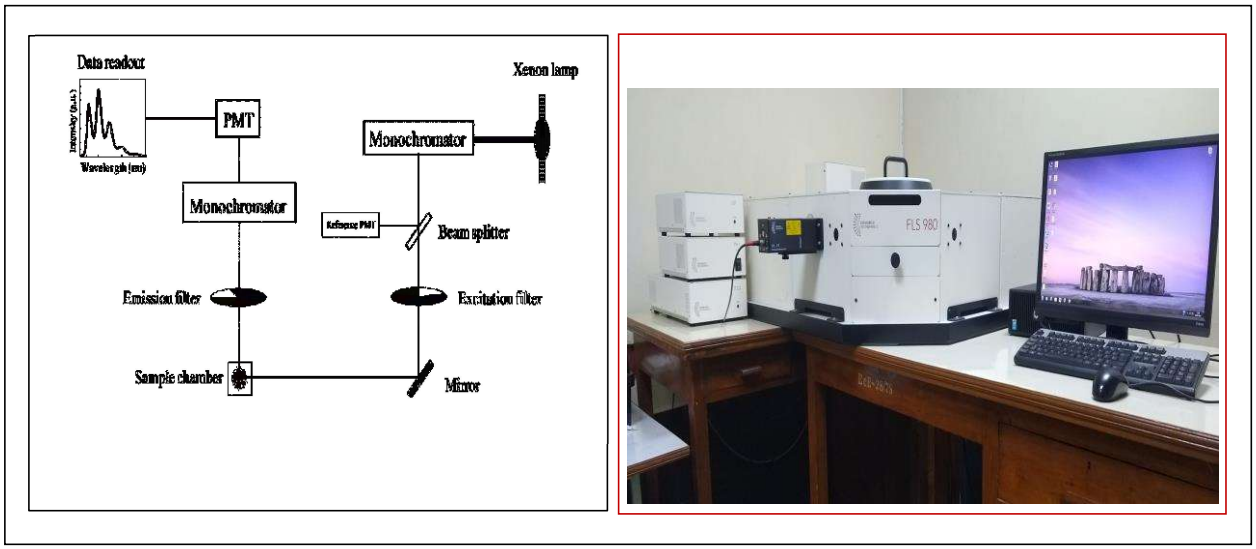

Figure 2.5 Schematic representation of working principle and photograph of fluorescence spectrophotometer.

2.7.5. Time - Resolved Fluorescence Spectroscopy

To measure the life time of fluorescent materials, Time- resolved fluorescence spectroscopy is frequently used. The most advantageous properties of fluorescence life time are that it provides an absolute measurement and permit for a vigorous image of fluorescence. The fluorescence life time is a native molecular property and after diluting and concentrating the sample, its value does not change.

2.7.6. Fluorescence Decay

The fluorescent decay profile of CQDs was fitted by a tri-exponential function. Chi-square values and corresponding residual distribution were reduced to judge the best fit. The acceptable fit has a chi-square close to unity.

The fitting system of the fluorescence emission intensity decay $I_{(t)}$ uses a tri-exponential representation according to the following **equation 2.7**

$$I_{(t)} = B_1 \exp(- t / \tau_1) + B_2 \exp(-t / \tau_2) + B_3 \exp(-t / \tau_3) \quad \textbf{2.7}$$

Where τ_1 , τ_2 and τ_3 represents time constants of the three radiative decays channel and B_1, B_2 , B_3 are three corresponding amplitudes.

The following equation 2.8 was used to calculate the average life time-

$$< \tau > = \frac{B_1 \tau_1^2 + B_2 \tau_2^2 + B_3 \tau_3^2}{B_1 \tau_1 + B_2 \tau_2 + B_3 \tau_3} \quad \textbf{2.8}$$

In current research work, the fluorescence decay profile was acquired on instrument "Edinburgh FLS 980 fluorescence spectrophotometer" (Fig. 2.5).

2.7.7. X-ray Diffraction (XRD)

To study the texture, composition, structure and physical properties of the resources, the powerful analytical technique utilized is XRD. In a mixture of amorphous and crystalline materials, it provides in details about atomic spacing, lattice parameters, grain size and degree of crystallinity. These informations give in details regarding structure and properties of the materials. The functioning principle of XRD depends on constructive interference of monochromatic X−rays and sample crystallinity. This condition is possible only when Bragg's law is satisfied (Fig. 2.6), in which the wavelength of electromagnetic radiation related to the diffraction angle and the lattice spacing in a crystalline sample (Equation 2.9).

$$n\lambda = 2d\sin\theta \qquad \textbf{(2.9)}$$

Where, λ is the wavelength of X-rays, n is an integer value, d is interplanar distance and θ is the angle of diffraction.

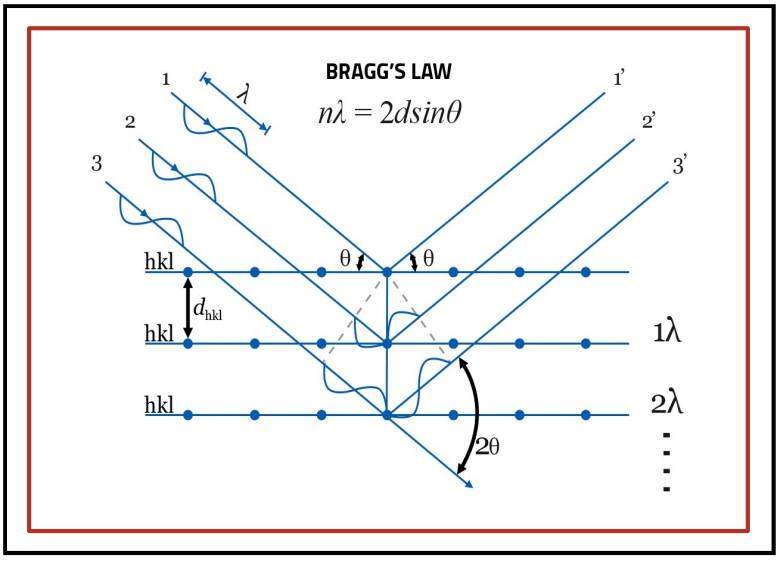

Figure 2.6 Diagrammatic representation of Bragg's Law.

In a usual XRD, the cathode ray tube is use to generate X-ray and the filtered monochromatic radiation collimated and intended toward the sample. Constructive interference i.e. diffracted ray are produces when the incident rays interact with the sample. Further, the diffracted X−rays are detected, processed and counted. Finally, attained the all possible directions of the diffraction lattice and scanned the sample throughout a range of angles of 2θ.

There are three fundamental components of X-ray diffractometers including X-ray tube, a sample holder, and an X-ray detector. By heating a filament in a cathode ray tube, electrons are produced which go faster toward a target by applying a voltage and bombarding the target materials by electrons. Further, characteristic X-ray spectra are obtained when electrons possess sufficient energy to displace inner shell electrons of the target materials. This spectrum includes numerous components, generally K_α and K_β. K_α consists of $K_{\alpha1}$ and $K_{\alpha2}$. The wavelength of $K_{\alpha1}$ is slightly shorter and twice the intensity as $K_{\alpha2}$.The wavelength $K_{\alpha1}$ and $K_{\alpha2}$ are adequately close. The most common target material for single-crystal diffraction is Copper. Subsequently, the produced X-rays are collimated and intended on the target molecules and with the rotation of the sample and detector, record the intensity of the reflected X-rays. The X-ray signal are detected and converted for count rate and on computer screen, final spectra are displayed (Fig.2.7).

In our research work, the P-XRD of samples was acquired on Mini Flex 600 (Rigaku, Tokyo, Japan) instrument (Fig 2.7). To generate Cu-Kα radiation (λ = 1.54059 Å), 40 kV voltage and 15 mA tube current was applied on the X-Ray tube. The NaI scintillator detector were used

to record the diffracted X-Rays and measure the XRD patterns at scan rate of 5°/min with step size of 0.02.

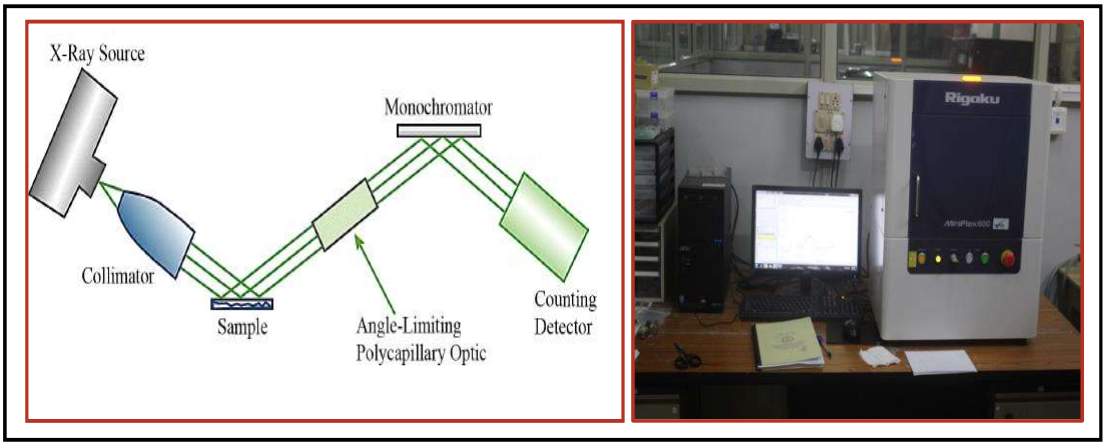

Figure 2.7 Illustration of working principle of XRD with its photograph.

2.7.8. X-ray Photoelectron Spectroscopy (XPS)

XPS is broadly utilized surface analysis technique since it gives helpful information about chemical state from the surface of the material. XPS not only explain the presence of elements within a sample but also explain what other elements they are bonded to. Approximately 5 nm is the average depth of analysis for an XPS measurement. The functioning principle of XPS study depends on irradiation of target material with X-ray of adequate energy in ultra high vacuum condition around 10^{-9}millibar (mbar). As a result of this, electrons in specific bound states undergo excitation. Few photo-ejected electrons scatter inelastically throughout the sample enroute to the surface, whereas others go through rapid emission and undergo no loss of energy. When these photo-ejected electrons undergo vacuum, electron analyzer collect them

which measures their kinetic energy. An electron energy analyzer generates an energy spectrum of intensity against binding energy. The specific element is corresponded by each outstanding energy peak on the spectrum. How much element present in sample, is identified by the intensity of the peaks. Numbers of atoms present in every element are recognized by peak area. By calculating the particular contribution of each peak area, the chemical composition is obtained.

The major components of a XPS spectrum consist of a source of X-rays, an Ultra-High Vacuum (UHV) stainless steel chamber with UHV pumps, monochromator, an electron energy analyzer, an electron detector system, an electron collection lens, and a moderate vacuum sample introduction chamber. Generally Al Kα or Mg Kα is utilized for the X-ray source. The diagrammatic illustration of XPS is given in **Figure 2.8**.

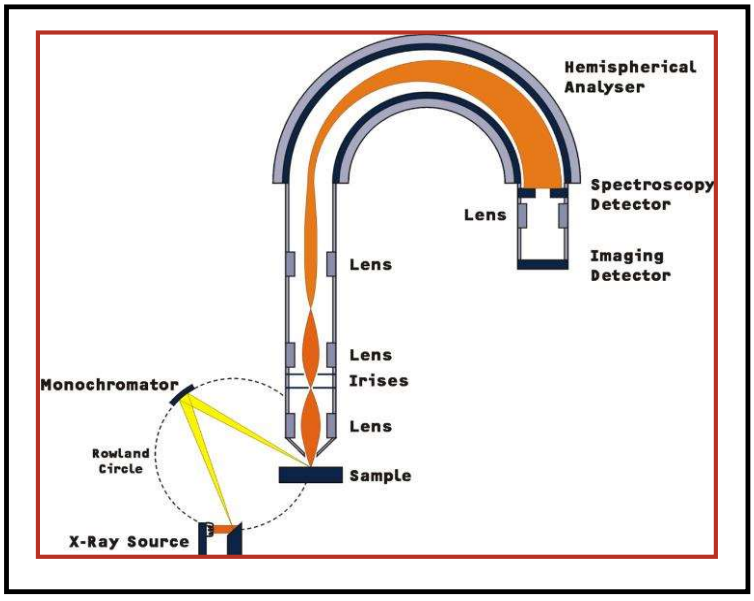

Figure 2.8 Working principles of XPS spectrum.

In our research work, XPS spectrum of the sample were carried out on "AMICUS, kratos, Analytical, A Shimadzu spectrometer" with Mg Kα excitation (1253.6 eV) radiation **(Figure 2.9).**

Figure 2.9 Typical photograph of XPS instrument.

2.7.9. Zeta Potential

The potential developed between the fixed layer and diffused double layer is called Zeta potential. In other word, Zeta potential is the charge develops at the interface between a solid surface and its liquid medium. It is denoted by the Greek letter zeta (ζ), and the unit is volts (V) or millivolts (mV). The Key indicator of the stability of colloidal dispersions is the zeta potential. The zeta potential \magnitude denotes the degree of electrostatic repulsion among neighboring, equally charged particles in dispersion. The value of zeta potential normally varies from +100 mV to -100 mV. The major reason behind the dispersion, aggregation or flocculation is the zeta potential. Therefore, colloids with soaring zeta potential (positive or negative) are electrically

stabilized while colloids with small zeta potentials results in coagulate or flocculate. Consequently, it could be utilized to progress the formulation of emulsions, dispersions and suspensions. It is extremely affected by the pH of the solution. At low pH, its value is positive and at high pH negative. The functioning principle and the typical photograph of the zeta sizer are given in Fig. 2.10. In the present study, the zeta potential was calculated using Malvern Zeta sizer (Malvern Instruments, Ltd.).

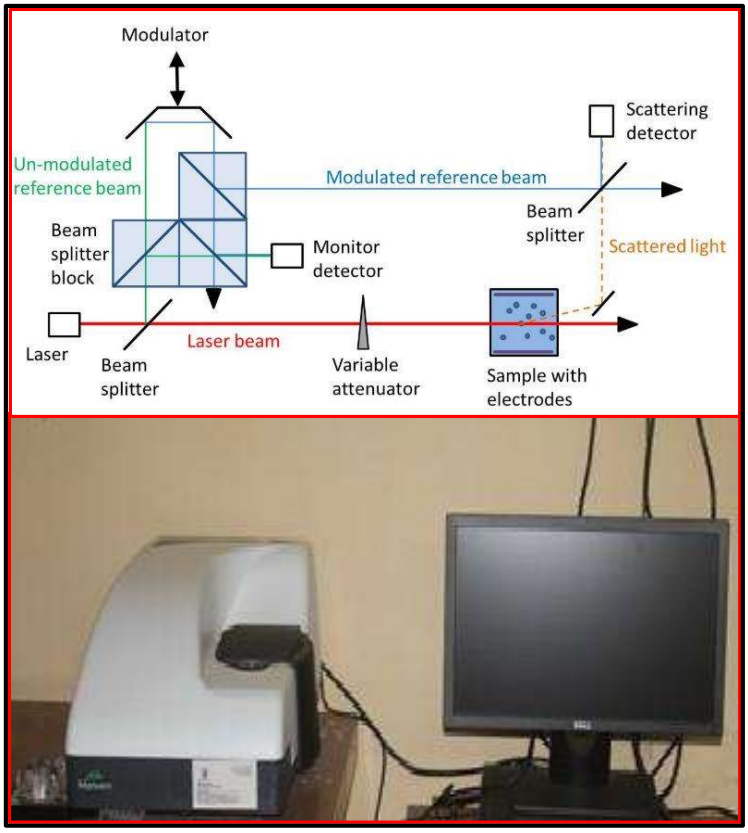

Figure 2.10 Working principles of Zeta sizer and its photograph.